

Structure of Lamellar Polysiloxane Induced by Interaction between Carboxylate (Alkanoate and Alkylsuccinate) and Aminosilane (Aminopropyl- and Aminoethylaminopropylsilanes)

Hitomi Nakajima,[1] Yasunori Oumi,[2] Tsuneji Sano,[2] and Hideaki Yoshitake*[1]

[1]Division of Materials Science and Chemical Engineering, Graduate School of Engineering, Yokohama National University, 79-5 Tokiwadai, Hodogaya-ku, Yokohama 240-8501

[2]Department of Applied Chemistry, Graduate School of Engineering, Hiroshima University, 1-4-1 Kagamiyama, Higashi-Hiroshima 739-8527

Received June 5, 2009; E-mail: yos@ynu.ac.jp

We demonstrate that the dehydration condensation of 3-aminopropylsilane (APTES) and 3-(2-aminoethyl)aminopropylsilane (AeAPTES) in the presence of alkylsuccinate and alkanoic acid provide layered polysiloxanes where the interlayer is filled with self-assembled carboxylate. Their structure was investigated by XRD, IR, and ^{29}Si NMR. Lamellar solids were successfully obtained by the combination of monocarboxylate–APTES and dicarboxylate–AeAPTES, while the addition of alkanol and TEOS was necessary for the synthesis by cross combinations, dicarboxylate–APTES and monocarboxylate–AeAPTES. The series of lamellar solids with different interlayer distance are formed with alkylsuccinate and AeAPTES. The *d*-spacing is increased linearly with the number of carbons in the alkyl chain of surfactant. Only T^3 species is detected in the ^{29}Si NMR spectrum of hexadecylsuccinic acid–AeAPTES, implying that the structure of polysiloxane is a thin layer with complete condensation of silane molecules. This structural uniqueness is also supported by the IR bands due to Si–O–Si asymmetric vibration at 1132–1140 cm^{-1}, suggesting a large Si–O–Si angle. This is because an angle near 180° is necessary for the structure of a R–$SiO_{1.5}$ layer solid that has organic groups equally populated on both sides. The amount of Fe^{3+} sorbed in diaminoalkylpolysiloxanes was smaller than in monoaminoalkylpolysiloxane.

Mesostructured organic–inorganic materials have drawn considerable attention for several decades.[1–5] Among these functionalized hybrid materials, lamellar solids with structures induced by the interaction between an organic self-assembly in the interlayer and typically, the polymerized silsesquioxane sheet (R–$SiO_{1.5}$), have been intensively studied due to the variation, ease of synthesis, a defined mesostructure and chemical stability.[6–14] Amino functions have been widely used in the synthesis of this type of solid either as a terminal group in a long alkyl chain[15] or as a 3-aminopropyl function with[16,17] and without[18] the aid of surfactant micelles. The various structural analyses have revealed that these synthesized solids have defined chemical compositions and ordered structures. In addition to the attractive structural features, the amine functions of these lamellar materials provide the capacity of carbon dioxide absorption.[15]

We have recently demonstrated that the hydrothermal treatment of a mixture of equal amount of alkanoic acid and 3-aminopropyltriethoxylsilane (APTES) results in the formation of a well-ordered lamellar solid containing equimolar alkanoic acid and 3-aminopropyl function with negligible Si–C bond scission.[17] The composition implies a high amino group density and hence a high capacity for cation sorptions. In fact, the $C_{11}H_{23}COOH \cdot NH_2C_3H_6SiO_{1.5}$ sorbed 2.1 mmol g^{-1} of Fe^{3+}. The exchangeability of interlayer alkanoate micelles suggests the structural flexibility in the chemical bond between the amino and carboxyl functions in the polysiloxane and the alkanoates micelles, respectively. Although the pH conditions in the synthesis implies that the interaction between amino and carboxylate functions is crucial for the formation of a lamellar polysiloxane, it has not yet been elucidated whether the combination of other aminoalkylsilanes and other carboxylate head groups also provide similar mesostructural materials.

In this study, we synthesized lamellar polysiloxane solids with varying combinations of aminoalkyl silanes and alkanoic acids as shown in Scheme 1. Since attempts at synthesis by cross combination (i.e., monocarboxylate–diaminosilane and dicarboxylate–monoaminosilane) turned out to be fruitless, the addition of spacers into both carboxylate and silane was carried out. The effect of isolation by this addition on the structure of the surfactant head group and the amino function were characterized by IR spectroscopy. The capacity of Fe^{3+} sorption by these synthesized solids was also measured to compare the combinations of amino and carboxylate functions.

Experimental

Chemicals. 3-Aminopropyltriethoxysilane (APTES), 3-(2-aminoethylamino)propyltriethoxysilane (AeAPTES), lauric acid sodium salt (LAS) were purchased from Tokyo Chemical Industry Co., Ltd. Alkylsuccinic acids (C_nSA: octyl ($n = 8$), decyl ($n = 10$), dodecyl ($n = 12$), tetradecyl ($n = 14$), hexadecyl ($n = 16$), and octadecyl ($n = 18$) succinic acid) anhydrides and alcohols (C_nOH:

Published on the web October 8, 2009; doi:10.1246/bcsj.82.1313

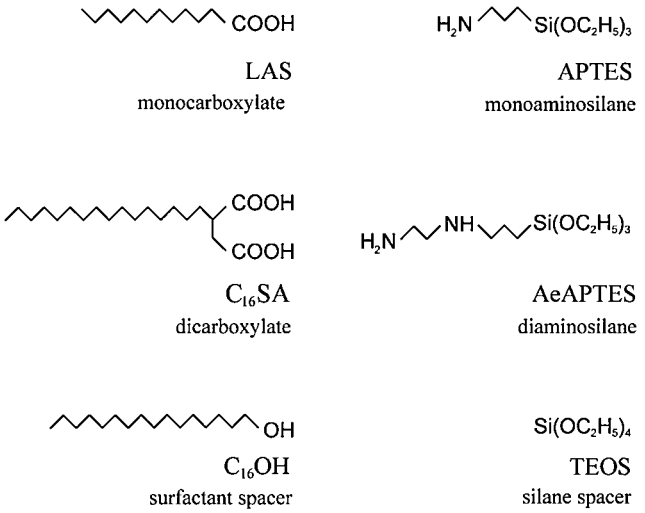

Scheme 1. Surfactants and silanes used for lamellar solids. The additive agents "spacers" are also indicated.

1-octanol ($n = 8$), 1-decanol ($n = 10$), 1-dodecanol ($n = 12$), 1-tetradecanol ($n = 14$), 1-hexadecanol ($n = 16$), and 1-octadecanol ($n = 18$)) were also obtained from Tokyo Chemical Industry except 1-hexadecanol purchased from Aldrich. Tetraethyl orthosilicate (TEOS) and sodium hydroxide were available from Tokyo Chemical Industry and Wako Pure Chemical Industries, respectively. These chemicals were used without further purification.

Preparation of LAS–APTES, LAS–AeAPTES–C_{16}OH–TEOS, C_{16}SA–APTES–C_{16}OH–TEOS, and C_{16}SA–AeAPTES–C_{16}OH–TEOS. We prepared materials in three series. These materials are listed in Table S1 in Supporting Information.

For the combination of mono- and dicarboxylates with mono- and diaminosilanes, we tried to synthesize solids from the following acid–aminosilane combinations: LAS–APTES, LAS–AeAPTES, C_{16}SA–APTES, and C_{16}SA–AeAPTES. LAS–APTES was prepared according to the literature.[17] The combinations of LAS–AeAPTES and C_{16}SA–APTES did not lead to solid products. With the addition of C_{16}OH and TEOS to the gel in these combinations, white precipitate was formed by the same preparation procedure as that for LAS–APTES and C_{16}SA–AeAPTES.

Hexadecanol, 32.36 g of water (1.80 mol), and 41.5 g of ethanol (0.90 mol) were added to LAS or C_{16}SA anhydride. The mixtures were stirred at 333 K until complete dissolution of alkanoate and alcohol. APTES or AeAPTES was added with 3.33 or 2.08 g of TEOS (0.016 or 0.01 mol, respectively) to this solution, followed by stirring for 1 h. After pH adjustment to 10.0, the solution mixture was transferred to a teflon bottle and heated at 373 K for 3 d. The solid was separated by filtration, washed and dried at 373 K for 7 d.

The molar ratios were LAS:APTES = 1:1 (LAS–APTES), LAS:AeAPTES:C_{16}OH:TEOS = 2:1:4:4 (LAS–AeAPTES–C_{16}OH–TEOS), C_{16}SA:APTES:C_{16}OH:TEOS = 1:2:4:4 and 1:2:1:1 (C_{16}SA–APTES–C_{16}OH–TEOS), and C_{16}SA:AeAPTES:C_{16}OH:TEOS = 1:1:1:1 (C_{16}SA–AeAPTES–C_{16}OH–TEOS).

Preparation of C_nSA–AeAPTES ($n = 8$, 10, 12, 14, 16, and 18). We hydrothermally synthesized solids without alkanol and TEOS for the series of dicarboxylate (C_nSA)–diaminosilane (AeAPTES). 32.36 g of water and 41.5 g of ethanol were added to 0.005 mol of C_nSA. The mixture was stirred at 333 K until complete dissolution. 1.32 g of AeAPTES was added to this solution, followed by stirring for 1 h. The molar ratio of C_nSA:AeAPTES = 1:1. After pH adjustment to 10.0, the solution mixture was transferred into a teflon bottle and heated at 373 K for 3 d. The precipitate was separated by filtration, washed, and dried at 373 K for 7 d.

Preparation of C_nSA–AeAPTES–C_nOH–TEOS ($n = 8$, 10, 12, 14, 16, and 18). In order to explore the effects by dilution of self-assembly of alkanoate with alkanol, we hydrothermally synthesized solids from mixtures of C_nSA, AeAPTES, C_nOH, and TEOS keeping the molar ratio C_nSA:AeAPTES:C_nOH:TEOS = 1:1:1:1. A typical procedure is as follows. 32.36 g of water (1.80 mol) and 82.92 g of ethanol (1.80 mol) were added to 0.01 mol of C_nSA. After the addition of 0.01 mol of C_nOH and 2.08 g of TEOS, the mixture was stirred at 333 K until complete dissolution. 2.64 g of AeAPTES was added to this solution, followed by stirring for 1 h. After pH adjustment to 10.0, the solution mixture was transferred to a teflon bottle and heated at 373 K for 3 d. The solid was separated by filtration, washed, and dried at 373 K for 7 d.

Structural Analysis. All solids were analyzed by X-ray diffraction (XRD) using a RINT 2200 diffractometer (Rigaku Co.) with Cu Kα radiation (40 keV and 20 mA). The Fourier transform-infrared spectra of solid powder dispersed in KBr pellets were measured with a JASCO FT/IR-4200 spectrometer. Proton-decoupled ^{29}Si MAS NMR spectra were measured using a Brucker Avance DRX-400 spectrometer at 79.5 MHz with a sample spinning rate of 5 kHz. A 7 mm-diameter zirconia rotor was used. The spectra were accumulated with 5.0 μs pulses, 20 s recycle delay, and 1000 scans.

Sorption of Iron(III) Ion. A 10 mL solution of Fe^{3+} in ethanol (179 mM prepared with iron(III) chloride hexahydrate, $FeCl_3 \cdot 6H_2O$, an excess in comparison to the number of amine functions in the testing powders) was added to 0.05 g of LAS–APTES, LAS–AeAPTES–C_{16}OH–TEOS, C_{16}SA–APTES–C_{16}OH–TEOS, and C_{16}SA–AeAPTES–C_{16}OH–TEOS and the mixture was stirred at room temperature for 48 h. The concentration of Fe^{3+} before and after the sorption was determined by inductively coupled plasma-atomic emission spectroscopy (ICP-AES, ICP-8000E, Shimadzu). After vacuum filtration, the solid was dried in air at 373 K and elemental analysis was carried out with energy dispersive X-ray spectrometry equipped with a JSM-6230 LA scanning electron micrometer (JEOL).

Results and Discussion

Combinations of Surfactant and Silane Molecules with One or Two Functional Groups, LAS–APTES, LAS–AeAPTES–C_{16}OH–TEOS, C_{16}SA–APTES–C_{16}OH–TEOS, and C_{16}SA–AeAPTES–C_{16}OH–TEOS. Figure 1 shows XRD of the products from the mixtures of carboxylates (mono- or di-), aminosilane (mono- or di-), alkanol, and TEOS as well as the data of LAS–APTES. The dehydration polymerization of APTES in the presence of *n*-alkyl monocarboxylate (RCOOH) results in the formation of a lamellar structure where the LB film like micelle in the interlayer combines polysiloxane sheets.[16,17] This structure has been relatively well analyzed due to the simple composition, i.e., $RCOOH \cdot NH_2CH_2CH_2CH_2$-$SiO_{1.5}$, and an easy comparison with the vast LB films data.[17] LAS–APTES in this study provided the same XRD pattern as in the previous studies. However, the simple expansion from mono- to dicarboxylic acid and amine molecules was not successful in the syntheses with the combination of C_{16}SA–APTES and with that of LAS–AeAPTES. Although we

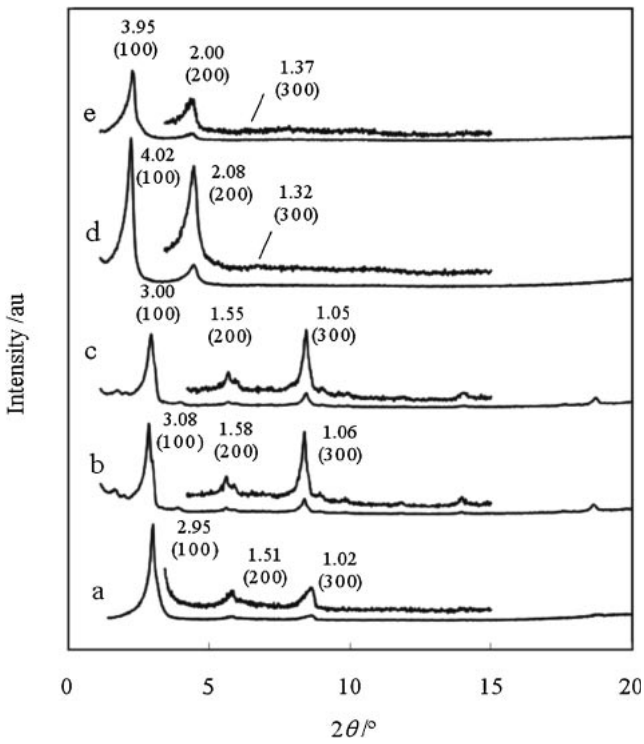

Figure 1. XRD patterns of polysiloxanes prepared by various combinations of carboxylates and aminoalkylsilanes. Solids from the mixture of (a) LAS:APTES = 1:1, (b) LAS:AeAPTES:C_{16}OH:TEOS = 2:1:4:4, (c) C_{16}SA:APTES:C_{16}OH:TEOS = 1:2:4:4, (d) C_{16}SA:APTES:C_{16}OH:TEOS = 1:2:1:1, and (e) C_{16}SA:AeAPTES:C_{16}OH:TEOS = 1:1:1:1. The numbers marked at peaks are *d*-value in nm and the indices in parentheses.

examined various conditions, we did not obtain solid products. Considering the fact that pH <10.5, where both carboxylate and amine would be ionized in homogeneous solution, is critical for the synthesis of these lamellar solids, the failure of a structural match between carboxylate and amine is likely the reason why our attempts were unsuccessful. The isolation of the functional groups possibly facilitates the interaction between these unmatched carboxylate–amine combinations. Therefore, we prepared the materials in the presence of alkanol and TEOS for the dilution of carboxyl and amino functions, respectively. As we have considered that the interaction between carboxyl and amine groups is an important factor for the formation of the characteristic solid structure, the same number of COOH and amine (NH_2– and –NH–) functions were loaded in the synthetic gel. As a consequence, equimolar alkanol and TEOS were used where necessary. We confirmed that a simple mixture of C_{16}OH and TEOS did not provide any solid products by the same hydrothermal synthesis, suggesting negligible interaction between TEOS and alkanol. The dehydration polymerization of AeAPTES in the presence of C_{16}SA in contrast provided lamellar solid (vide infra) likely that of APTES in the presence of LAS.

With the addition of alkanol and TEOS, clear peaks indexed with (100), (200), and (300) diffractions are observed for all combinations of carboxylates and aminosilanes, suggesting that these materials are as lamellar as LAS–APTES, where LB film-like self-assembly is formed in the interlayer of polysiloxanes. The lattice plane distance of LAS–AeAPTES–C_{16}OH–TEOS (2:1:4:4) and C_{16}SA–APTES–C_{16}OH–TEOS (1:2:4:4) is almost the same (Figures 1b and 1c), implying that the number of functions in a surfactant and a silane is not important for the layer distance, though solid is not obtained without a combination of carboxyl and amine functions. An experiment with decreasing C_{16}OH (and TEOS) in the gel, from LAS–AeAPTES–C_{16}OH–TEOS (4:2:8:8) to LAS–AeAPTES–C_{16}OH–TEOS (2:4:8:8), is consistent with this assumption. When equimolar surfactants were used for C_{16}SA–APTES–C_{16}OH–TEOS (i.e., C_{16}SA:C_{16}OH = 1:1, Figure 1d), the lattice plane distance changed from 3.00 to 4.02 nm and again the difference from the lamellar solid from dicarboxylate–diamine combination with the same mixing ratio (C_{16}SA–AeAPTES–C_{16}OH–TEOS with C_{16}SA:C_{16}OH = 1:1, Figure 1e) is small (0.05 nm). The above results imply that the alkyl chain length of alkanol determines the interlayer distance when it has a longer chain than carboxylate and the size of diamine functions do not influence significantly the distance. The origin of enlargement of the plane distance with the surfactant composition is not clear.

The IR spectra of these solids are depicted in Figure 2, where the regions for C–H and C=O stretching vibrations are separately shown. The bands at 2955–2956 and at 2871–2873 cm^{-1} are assigned to CH_3-asymmetric, $\nu_{as}(CH_3)$, and CH_3-symmetric, $\nu_s(CH_3)$, stretching vibrations, respectively. No clear shift was found for these bands. The band for methylene symmetric vibration, $\nu_s(CH_2)$, appears at nearly identical positions (2849–2852 cm^{-1}). In contrast, the antisymmetric vibration, $\nu_{anti}(CH_2)$, which appear in ca. 2920 cm^{-1}, shifts from 2922 cm^{-1} for the solid from LAS surfactant (Figure 1a) to 2917 cm^{-1} for that from C_{16}SA–C_{16}OH (Figures 1d and 1e). Interestingly, the band for the solid from LAS–C_{18}OH mixed surfactant appears at the highest position, 2924 cm^{-1}. The antisymmetric stretching vibration of methylene C–H has been used as a measure for the conformational degree of freedom of alkyl groups in LB film-like micelles.[6,17,19] The observations, $\nu_{anti}(CH_2)$ at 2925 and 2917 cm^{-1} in liquid alkane (dodecane) and high density polyethylene, respectively, are two distinct conformational states in conventional condensed states. Most alkyl chains in the latter solid are generally believed to be in all trans conformations. The agreement of the band position of $\nu_{anti}(CH_2)$ suggests that the alkyl groups in the interlayer of the solid from C_{16}SA–C_{16}OH mixed surfactant are as dense as in high density polypropylene and arranged in all-trans conformation. The higher $\nu_{anti}(CH_2)$ in the solid from LAS–APTES than in that from C_{16}SA–C_{16}OH is reasonably explained by the difference in alkyl chain length; long alkyl chains interact with each other strongly. The highest $\nu_{anti}(CH_2)$ in solid from LAS–C_{18}OH mixture implies that mixing different alkyl chains causes the formation of a weak self-assembly state. The shoulder band at 2938 cm^{-1} found in solids from LAS and from LAS–C_{16}OH mixed surfactant is assigned to the Fermi resonance of the methyl symmetric stretch.[19]

The bands at 1463–1468 and ca. 1440 cm^{-1} are due to $\delta_s(CH_2)$ and $\delta_{as}(CH_3)$, respectively. The absorptions around 1700 and 1405 cm^{-1} are attributed to carbonyl stretching and O–H bending vibrations of non-dissociative COOH, respec-

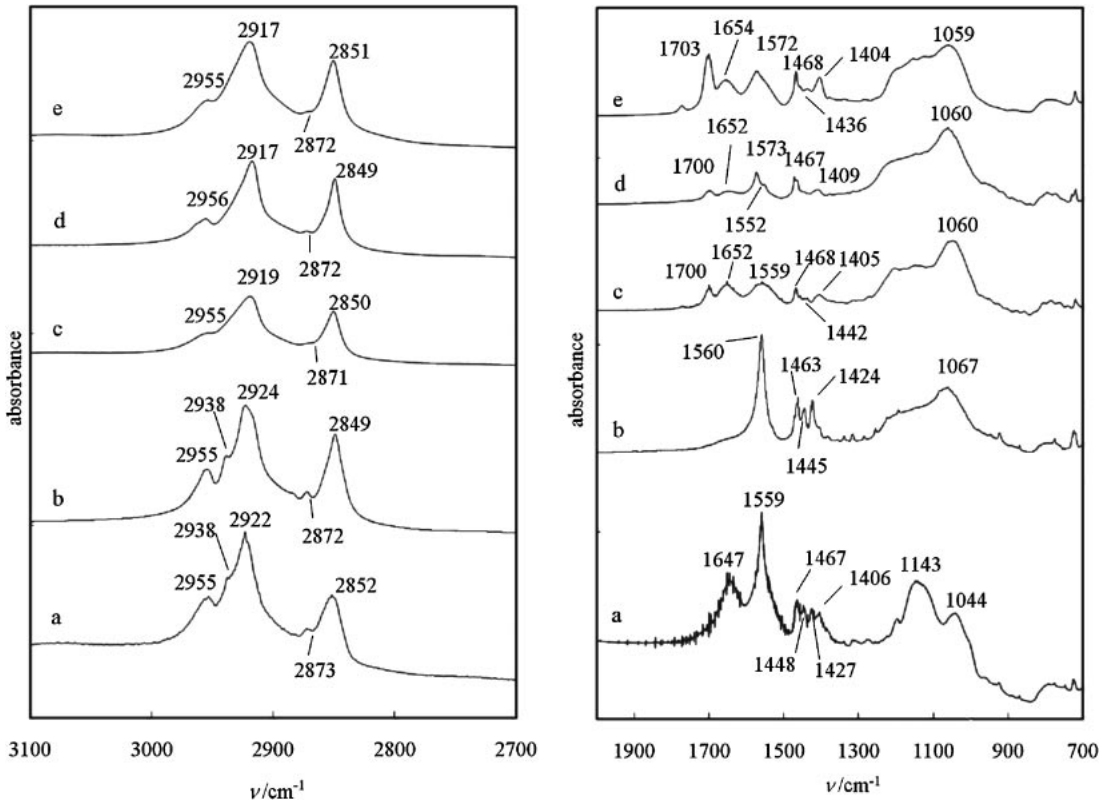

Figure 2. Infrared spectra of polysiloxanes prepared by various combinations of carboxylates and aminoalkylsilanes. Solids from the mixture of (a) LAS:APTES = 1:1, (b) LAS:AeAPTES:C_{16}OH:TEOS = 2:1:4:4, (c) C_{16}SA:APTES:C_{16}OH:TEOS = 1:2:4:4, (d) C_{16}SA:APTES:C_{16}OH:TEOS = 1:2:1:1, and (e) C_{16}SA:AeAPTES:C_{16}OH:TEOS = 1:1:1:1.

tively. The absorptions at 1559–1572 and ca. 1425 cm^{-1} are attributed to antisymmetric and symmetric vibrations of dissociative $–COO^-$. The distinct signals for $–COO^-$ appear in the solids from LAS, while stronger signals for –COOH than those for $–COO^-$ are observed in those from C_{16}SA. This switching of carboxyl ionization is probably due to the density/distance of neighboring groups. Since ionic interaction is isotropic and –OH groups are not ionized, it is likely that neighboring carboxyl groups promote the dissociation of –COOH, which is accompanied by the protonation of amino groups. This hypothetical model is supported by change in the intensity of bending vibration of $–NH_2$, which appears around 1650 cm^{-1}. The growth and decline of this peak agree well with those of –COOH. Furthermore, comparing the two C_{16}SA–APTES–C_{16}OH–TEOS solid with different compositions (Figures 2c and 2d), the peak due to $–COO^-$ (at 1573 cm^{-1}) is more distinct in solid prepared with less C_{16}OH (Figure 2d) than in the spectrum for solid prepared with more C_{16}OH (Figure 2c), supporting the model.

The broad absorption in the region of 1000–1200 cm^{-1} is due to asymmetric vibration of Si–O–Si bonds. The distinct peak at 1143 cm^{-1} observed in LAS–APTES becomes insignificant in lamellar solids prepared with TEOS. This peak is discussed in the following section.

The results of elemental analysis were C, 56.5; N, 4.31 wt % for LAS–APTES, C, 56.0; N, 1.83 wt % for LAS–AeAPTES–C_{16}OH–TEOS, C, 53.9; N, 1.27 wt % for C_{16}SA–APTES–C_{16}OH–TEOS (1:2:4:4), C, 50.2; N, 3.53 wt % for C_{16}SA–APTES–C_{16}OH–TEOS (1:2:1:1), and C, 57.7; N, 4.28 wt % for C_{16}SA–AeAPTES–C_{16}OH–TEOS. The respective carbon to nitrogen ratios (mol/mol) were 15.4, 35.7, 49.4, 16.6, and 15.7. Calculation assuming that the composition of the solid is the same as the mixing ratio of surfactants and silanes in its preparation provided the theoretical values C/N = 15, 40.5, 43, 19, and 18.5, respectively. The experimental data agree with the theoretical values within ca. 15%. The presence of SiO_4 unit in C_{16}SA–AeAPTES–C_{16}OH–TEOS was confirmed by ^{29}Si NMR. The population of Q^4 species in the observed T^2, T^3, Q^3, and Q^4 species was calculated to be 40%.

Lamellar Solid from Dicarboxylates and Diaminosilanes, C_nSA–AeAPTES. The XRD of C_nSA–AeAPTES (n = 8, 10, 12, 14, 16, and 18) are depicted in Figure 3. The lamellar pattern with three distinct peaks can be found in the data from dodecyl- (n = 12) to octadecyl- (n = 18) succinic acids. The (300) diffraction is not clearly observed in the signal from the solids prepared with octyl- and decylsuccinic acids. Nevertheless, we indexed the most distinct peak with (100) and calculated lattice plane distance from its position. The plot of d-spacing against the number of carbons in the alkyl chain of surfactant is shown in Figure 4. The data are fitted well with $d(100)/\mathrm{nm} = 0.200n + 0.800$, where n is the number of carbon atoms in the alkyl chain. The drastic decline in the periodic order when n is smaller than 10 agrees with no solid formation in the synthesis with $C_nH_{2n+2}COOH$ ($n < 10$) and APTES, though a good lamellar structure was obtained using LAS, MAS, PAS, and SAS (n = 11, 13, 15, and 17, respectively).[17]

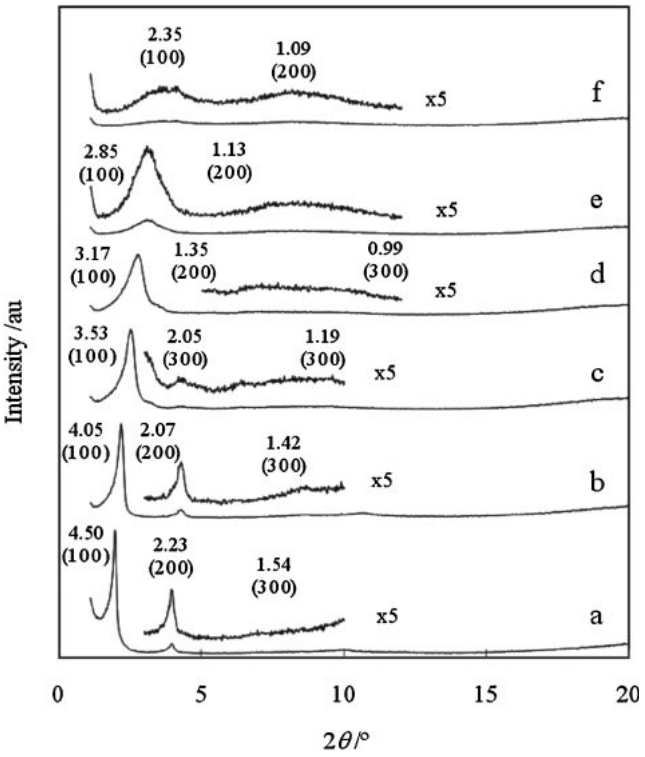

Figure 3. XRD patterns of lamellar polysiloxanes prepared by the combination of various alkyl succinic acids (C_8SA–C_{18}SA) with equimolar 3-(2-aminoethyl)aminopropylsilane. Alkyl succinic acids used are (a) C_{18}SA, (b) C_{16}SA, (c) C_{14}SA, (d) C_{12}SA, (e) C_{10}SA, and (f) C_8SA. The numbers marked at peaks are *d*-value in nm and the indices in parentheses.

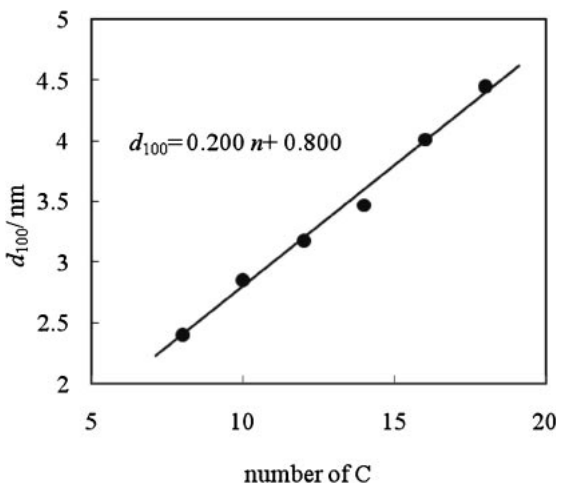

Figure 4. *d*-Spacing against number of carbon atoms in the alkyl chain of alkyl succinic acids in lamellar polysiloxanes prepared with alkyl succinic acids (C_8SA–C_{18}SA) and equimolar 3-(2-aminoethyl)aminopropylsilane.

However, $d(100)/\mathrm{nm} = 0.166n + 1.082$ has been reported for the series of monocarboxylate.[17] In the all-trans conformation, the length of alkyl chain would increase by 0.25 nm per carbon atom. The lower than expected slope value for all-trans conformation is possibly caused by a large tilt angle of the interlayer micelle, interdigitation varying linearly with the chain length and mixed conformational state (i.e., gauche and trans). Interdigitation is less likely in these carboxylate–aminoalkyl polysiloxane lamellar solids, because it will lower the population of trans conformation and linearity in the $d(100)$–n plots. The existence of a tilt angle is most likely the mechanism for the slope and its difference in the series of monocarboxylates is probably due to the different functional groups and higher population of trans conformations in C_nSA–AeAPTES solids than in monocarboxylate–monoaminoalkyl polysiloxane lamellar solids.

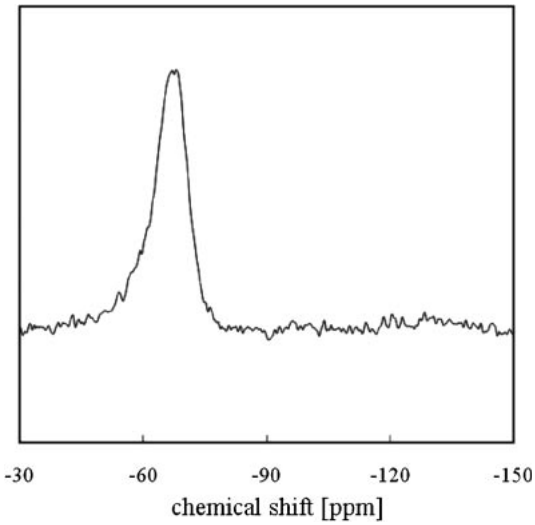

Figure 5. ^{29}Si CPMAS NMR spectrum of C_{16}SA–AeAPTES.

Figure 5 shows the ^{29}Si MAS NMR spectrum of C_{16}SA–AeAPTES. A single peak at −66.2 ppm was found, which is attributed to T^3 species. The absence of T^2 and Q^n ($n = 1$, 2, 3, and 4) species implies no significant formation of Si–OH and bond scission of Si–C, respectively. This distinct spectral feature establishes evidence for a complete dehydration condensation in the hydrothermal synthesis and successive drying process. The elemental analysis of nitrogen in C_{16}SA–AeAPTES was 4.40 mmol g^{-1}, which agrees with the formula $C_{16}H_{33}(COOH)CHCH_2COOH$–$NH_2C_2H_4NHC_3H_6SiO_{1.5}$ (N: 4.04 mmol g^{-1}).

The IR spectra of C_nSA–AeAPTES are shown in Figure 6. As discussed above, the peaks at 2955–2959 and 2871–2873 cm^{-1} are due to CH_3-groups in alkylsuccinic acids. Similarly, the bands at 2918–2927 and 2850–2854 cm^{-1} are assigned to $\nu_{anti}(CH_2)$ and $\nu_s(CH_2)$, respectively. The position of $\nu_{anti}(CH_2)$ gradually shifts from 2918 (for C_{18}SA–AeAPTES) to 2927 cm^{-1} (for C_8SA–AeAPTES). This transition of the band position is clearly attributed to the lowering of density of alkyl chains due to the shortening of the length. Since the gauche conformation decreases with the effective alkyl chain length and with the thickness of micelle that is formed with the surfactant, this effect could work to raise the slope in $d(100)$ vs. n plot. Considering that $\nu_{anti}(CH_2)$ of liquid alkane and high density polyethylene are 2925 and 2917 cm^{-1}, respectively, the shift in $\nu_{anti}(CH_2)$, which is caused by changing n from 8 to 18, $\Delta\nu_{anti}(CH_2) = 9\,\mathrm{cm}^{-1}$, is surprisingly large.

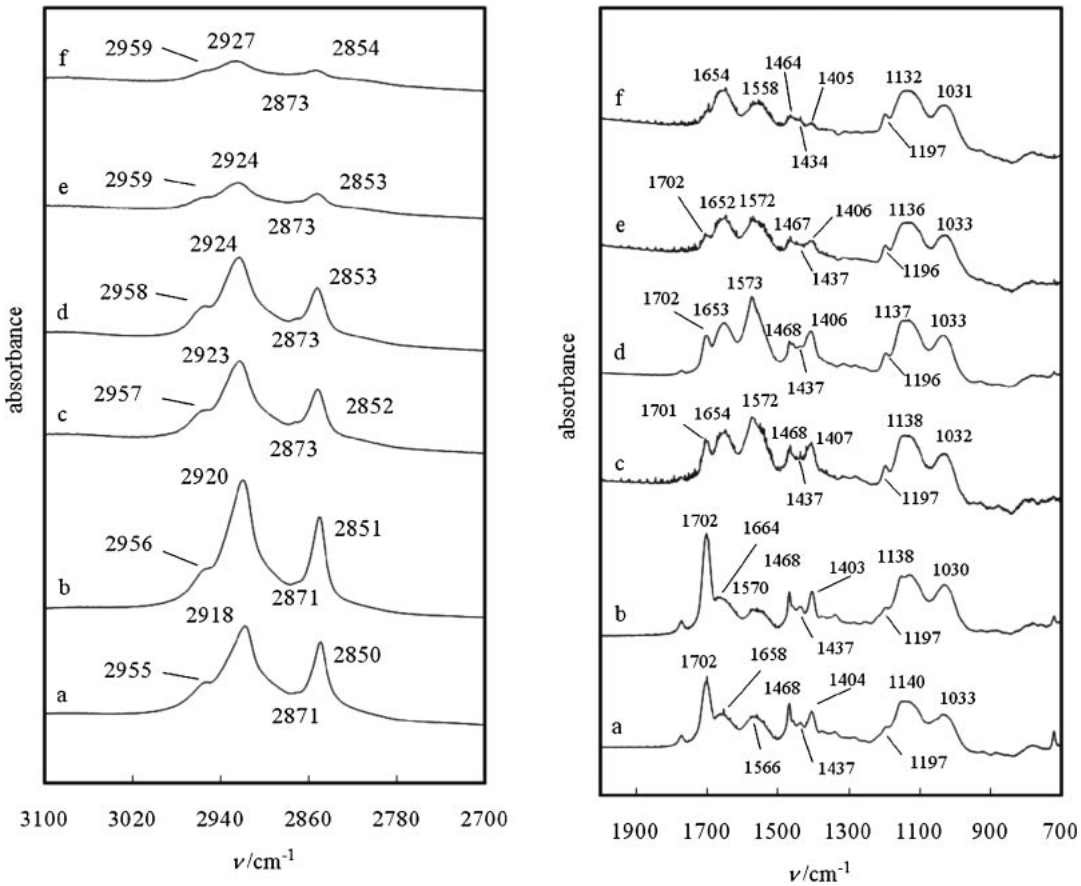

Figure 6. Infrared spectra of lamellar polysiloxanes prepared by the combination of various alkyl succinic acids (C_8SA–C_{18}SA) with equimolar 3-(2-aminoethyl)aminopropylsilane. Alkyl succinic acids used are (a) C_{18}SA, (b) C_{16}SA, (c) C_{14}SA, (d) C_{12}SA, (e) C_{10}SA, and (f) C_8SA.

The assignment of the bands in the region 700–1900 cm^{-1} is the same as in Figure 2. According to the decrease of the number of carbon atoms in the alkyl chain, the intensity of the band at 1702 cm^{-1} gradually decreases, while that at 1558–1573 cm^{-1} increases. As already discussed, these absorptions are attributed to the C–O stretching mode of –COOH and $–COO^-$, respectively. Since highly dense carboxyl and amino groups have a tendency to be ionized, this alternation of the band intensities suggests that alkylsuccinic acid with a short alkyl chain provides a large space for a carboxyl group. This is consistent with the assumption of a large population of gauche conformation in the interlayer self-assembly, which is suggested by the position of $\nu_{anti}(CH_2)$. Succinic acid has two carboxyl groups connected with –CHR–CH_2– and the orientation of these functions is more flexible than that in monocarboxylates. This flexibility may be effective to change the ionization state of carboxyl function. The band around 1405 cm^{-1}, which is attributed to carboxyl –OH, shows intensity changing with the C=O stretching vibration of –COOH.

The twin bands at 1030–1033 and 1132–1140 cm^{-1} are assigned to the asymmetric stretching motion of different Si–O–Si oxygen bridges. This vibration for a simple alkyldisiloxane is typically positioned between 1020 and 1125 cm^{-1}. The large blue shift from the positions of alkyldisiloxane suggests a large Si–O–Si bond angle. Using a typical force constant for Si–O–Si vibrations for silica, $f_r = 5.943 \times 10^{-18}$ J $Å^{-2}$ (ignoring the difference between Si–O and Si–C on the neighboring Si–O), the angle of Si–O–Si for the band $\nu_{as}(SiOSi) = 1044–1067\ cm^{-1}$ in Figure 2 and 1030–1033 cm^{-1} in Figure 6 is calculated to be $\theta = 137–144$ and 129–130°, respectively.[20] This range of angle is found in the center of the Si–O–Si angle distributions proposed for amorphous silica.[21,22] However, the bond angles for the bands at 1143 (Figure 2) and 1132–1140 cm^{-1} (Figure 6) correspond to $\theta = 180$ and 165–173°, respectively, according to the same calculation. These angles are rare in the distributions for amorphous silica.

In C_nSA–AeAPTES, Si atoms in the polysiloxane layer have the structure R–Si(OSi–)$_3$ (from ^{29}Si NMR) and the amine functions interact with COOH of the surfactant self-assembly to form a lamellar structure (from XRD). Such structure is geometrically possible when all Si–O–Si angles are 180°. Consider the highest symmetry possible under these two conditions, all R–SiO_3 tetrahedral units make up six-membered rings with their organic groups on the other side of the neighboring tetrahedral units. In this hypothetical case, illustrated in Figure 7, the Si–O–Si angle is 180°. Such structure has been proposed for $ClNH_3C_3H_6SiO_{1.5}\cdot H_2O$ polysiloxane.[16] However, the observation of two bands in IR spectra (Figure 6) strongly suggests that the lamellar solids contain significant amounts of Si–O–Si bonds with an angle usually found in amorphous silica in addition to nearly linear

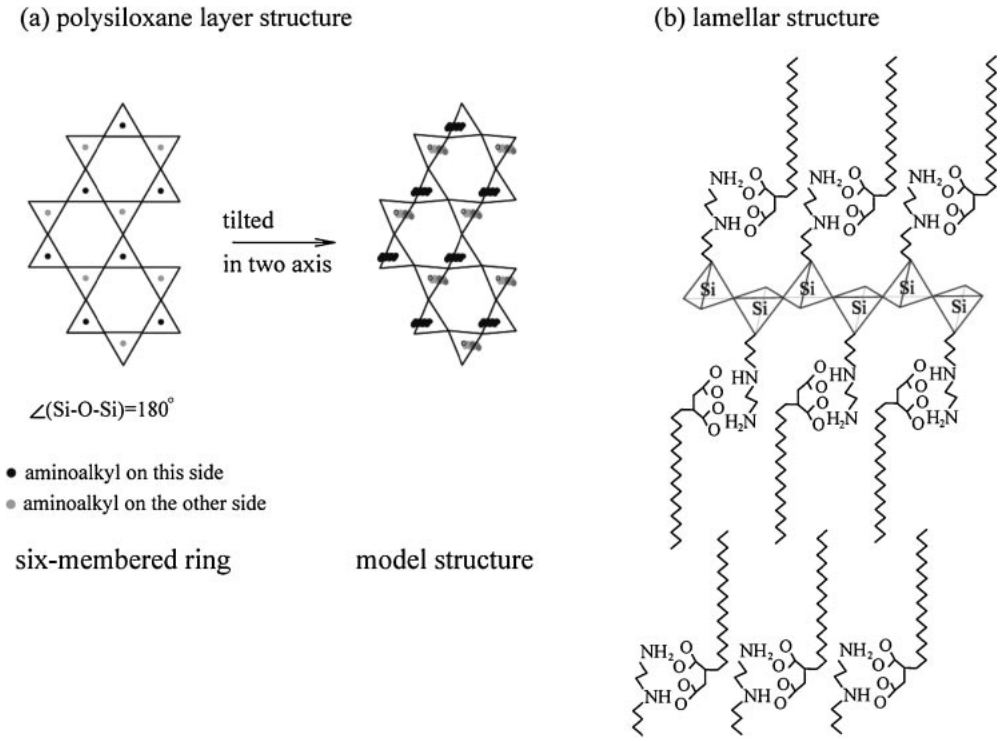

Figure 7. (a) A hypothetical six-membered ring structure composed of $RSiO_3$ trigonal pyramid units, where the angle of Si–O–Si is 180°,[16] and a model structure of the layer in C_nSA–AeAPTES, where the trigonal pyramid units are tilted in two axis. The trigonal pyramids with the aminoalkyl function on the same face are tilted nearly in the same way to bind with the surfactant self-assembly. (b) A model for carboxylate–amine interaction.

Si–O–Si. The tetrahedral units are tilted in two axis, one tilt is large and the other is small, and can explain the two different Si–O–Si angles. The angle Si–O–Si at 180° is clearly more unstable than that at lower angles such as 165–173°, considering the angle distributions in amorphous silica. This layer composed of tilted tetrahedrons is a likely model for C_nSA–AeAPTES. However, the six-membered ring is not identified in this study. The layer structure without large Si–O–Si angle has been observed in the crystalline β-$Na_2Si_2O_4$ built up with SiO_4^{4-} tetrahedral units, where the angles of Si–O–Si are 135.11, 136.50, and 137.11°,[23] while the IR bands assigned to asymmetric stretching appear at 1026, 1057, and 1084 cm^{-1}.[24] The lower band positions of crystalline β-$Na_2Si_2O_4$ than in Figure 6 suggest the presence of a large Si–O–Si angle in the lamellar polysiloxanes.

The perpendicular view of the model structure is also illustrated in Figure 7b. The tetrahedrons with the organic group on the same face of the layer are likely oriented to nearly the same direction to bind the C_nSA self-assembly. The head group of the surfactant and amino function are clearly larger than in LAS–APTES, possibly providing a more stable web of tetrahedrons in the polysiloxane layer by tilts than in LAS–APTES.

The shoulder band at 1196–1197 cm^{-1} in Figure 6 is assigned to the out of phase stretching mode of Si–O–Si.

Lamellar Solids from Dicarboxylates and Diaminosilanes with Dilution by Addition of Equimolar Alkanols and TEOS, C_nSA–AeAPTES–C_nOH–TEOS (n = 8–18). The XRD patterns of the solid formed from a mixture of equimolar C_nSA, AeAPTES, C_nOH, and TEOS are shown in Figure 8. The peaks can be assigned to (100), (200), and (300) diffractions only for $n = 16$ and 14. Although a clear diffraction peak is observed in the small angle region, the peak positions of C_{12}-, C_{10}-, and C_8-solids do not show the linear d(100) relationship with the number of carbon atoms as expected for the difference in alkyl chain length. The d-spacing is plotted against the number of carbons in alkyl chain in Figure S1. For $n = 18$, 12, 10, and 8, the lamellar structure is not developed well with the mixing surfactants in spite of the same length of alkyl chain. These solids provided no XRD patterns after careful calcinations. In the IR spectra shown in Figure 9, $\nu_{anti}(CH_2)$ in C_{18}- and C_{16}-solids are comparable with that of high density polyethylene and red shift with n is clearly found. The spectra also reveal that the peak at 1701–1703 cm^{-1} is more distinct than that at 1550–1570 cm^{-1} for all solids, and the change of the intensity with the length of alkyl chain is ambiguous. The latter finding is likely due to the separation of functions. From the IR data, the self-assembly of mixed surfactants is as dense as that prepared using only C_nSA, even though a developed layered structure is doubtful in C_{18}-, C_{12}-, C_{10}-, and C_8-solids. These results above imply that the comparison of the various combinations of carboxylate and aminosilane in Figures 1 and 2 may be done only when $n = 16$ and 14.

Sorption of Fe^{3+} in Various Lamellar Solids Prepared from Carboxylates and Aminosilanes. The amounts of Fe^{3+} ion sorbed in LAS–APTES, LAS–AeAPTES–C_{16}OH–TEOS, C_{16}SA–APTES–C_{16}OH–TEOS, and C_{16}SA–AeAPTES–C_{16}OH–TEOS are summarized in Table 1. LAS–APTES, which we reported previously,[17] sorbed the largest amount of

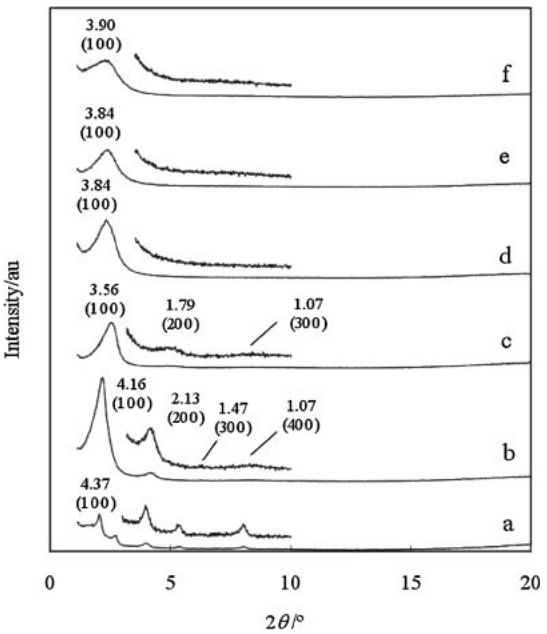

Figure 8. XRD patterns of lamellar polysiloxanes prepared by the combination of various alkyl succinic acids (C_8SA–C_{18}SA) with equimolar 3-(2-aminoethyl)aminopropylsilane (AeAPTES), alkanols (C_8OH–C_{18}OH) with the same alkyl chain and TEOS. Alkyl succinic acids used are (a) C_{18}SA, (b) C_{16}SA, (c) C_{14}SA, (d) C_{12}SA, (e) C_{10}SA, and (f) C_8SA. The numbers marked at peaks are *d*-value in nm and the indices.

Fe^{3+} per g-solid as well as per mole amine. By substituting APTES with AeAPTES, the uptake is reduced, not only per mole amine but also per mole aminoalkyl. This is probably due to the stronger bond between $NH_2C_2H_4NHC_3H_6$– and –COOH or $COOHCHCH_2COOH$ than $NH_2C_3H_6$–. This hypothesis can explain that we did not observe significant amount of Fe^{3+} sorption under the same experimental conditions in the C_nSA–AeAPTES lamellar solids, in which the functional groups are considered to be more tightly bound than C_{16}SA–AeAPTES–C_{16}OH–TEOS.

Table 1. Absorption of Fe^{3+} in the Lamellar Solids

Silicates	x_N /mmol g^{-1}	x_{Fe} /mmol g^{-1}	(x_{Fe}/x_N) /(mol g^{-1}/mol g^{-1})
LAS–APTES[a)]	3.5	2.1	0.60
LAS–AeAPTES–C_{16}OH–TEOS[b)]	7.3	0.73	0.10
C_{16}SA–APTES–C_{16}OH–TEOS[c)]	2.2	0.76	0.34
C_{16}SA–AeAPTES–C_{16}OH–TEOS[d)]	3.0	0.21	0.07

a) Synthesized with LAS and APTES (LAS:APTES = 1:1). b) Synthesized with LAS and AeAPTES in aid of C_{16}OH and TEOS (LAS:AeAPTES:C_{16}OH:TEOS = 2:1:4:4). c) Synthesized with C_{16}SA and APTES in aid of C_{16}OH and TEOS (C_{16}SA:APTES:C_{16}OH:TEOS = 1:2:4:4). d) Synthesized with C_{16}SA and AeAPTES in aid of C_{16}OH and TEOS (C_{16}SA:AeAPTES:C_{16}OH:TEOS = 1:1:1:1). e) x_N: amount of nitrogen in the solid and x_{Fe}: adsorption of Fe^{3+} ion in the solid.

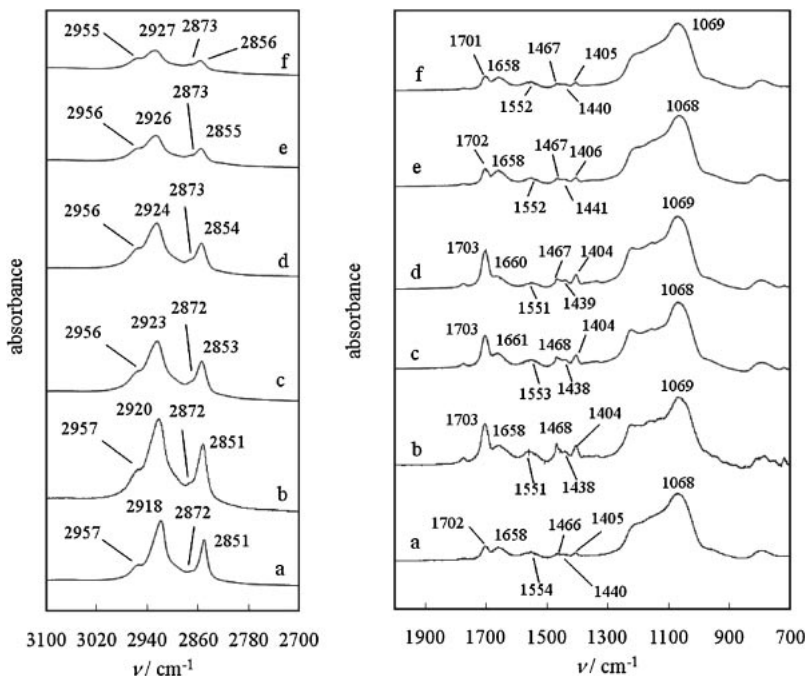

Figure 9. Infrared spectra of lamellar polysiloxanes prepared by the combination of various alkyl succinic acids (C_8SA–C_{18}SA) with equimolar 3-(2-aminoethyl)aminopropylsilane (AeAPTES), alkanols (C_8OH–C_{18}OH) with the same alkyl chain and TEOS. Alkyl succinic acids used are (a) C_{18}SA, (b) C_{16}SA, (c) C_{14}SA, (d) C_{12}SA, (e) C_{10}SA, and (f) C_8SA.

Conclusion

Lamellar polysiloxanes where the interlayer is composed of self-assembled surfactants were synthesized using monocarboxylates and dicarboxylates as anion surfactant and APTES (monoaminosilane) and AeAPTES (diaminosilane) as silane. The combinations of monocarboxylate–monoaminosilane and dicarboxylate–diaminosilane provided good lamellar solids, while the cross combinations, dicarboxylate–monoaminosilane and monocarboxylate–diaminosilane, needed the addition of alkanol and TEOS for the formation of layered structure. The IR spectroscopy revealed that the carboxylate group was ionized when the functional groups were densely populated in the solid. This was correlated with the band position of antisymmetric stretching vibration of $-CH_2-$ groups, a marker sensitive to the packing density of alkyl chains in Langmuir-type micelles. The series of lamellar solids were successfully synthesized with alkylsuccinic acids (C_nSA, dicarboxylates) and AeAPTES. The lattice plane distance $d(100)$ of lamellar solids synthesized with dicarboxylates (C_nSA,) and AeAPTES was linearly increased with the number of carbons in the alkyl chain in C_nSA. Only T^3 species was detected in the ^{29}Si NMR spectrum of C_{16}SA–AeAPTES, implying that the polysiloxane consists of two-dimensional solid. This structural uniqueness was also supported by two infrared absorption bands due to the asymmetric vibration of Si–O–Si: 1132–1140 and 1030–1033 cm^{-1}. The latter band position is extremely high, suggesting a large Si–O–Si bond angle unusual in amorphous silica. An angle near 180° is necessary for the structure of $R–SiO_{1.5}$ layered solid that has organic groups equally on both faces. The amount of Fe^{3+} sorbed in diaminoalkylpolysiloxanes was smaller than in LAS–APTES.

We would like to thank Profs. K. Ota and S. Mitsushima for their assistance in using ICP-AES. This study has been financially supported by Grant-in-Aid for Scientific Research by JSPS.

Supporting Information

Summary and synthesis conditions (Table S1) and *d*-spacing against number of atoms in the alkyl chain (Figure S1). This material is available free of charge on the web at http://www.csj.jp/journals/bcsj/.

References

1 H. Yoshitake, *New J. Chem.* **2005**, *29*, 1107.
2 D. Trong On, D. Desplantier-Giscard, C. Danumah, S. Kaliaguine, *Appl. Catal., A* **2003**, *253*, 545.
3 A. Tuel, *Microporous Mesoporous Mater.* **1999**, *27*, 151.
4 R. J. P. Corriu, A. Mehdi, C. Reyé, *J. Mater. Chem.* **2005**, *15*, 4285.
5 F. Zheng, R. S. Addleman, C. L. Aardahl, G. E. Fryxell, D. R. Brown, T. S. Zemanian, in *Environmental Applications of Nanomaterials, Synthesis, Sorbents and Sensors*, ed. by G. E. Fryxell, G. Cao, Imperial College Press, London, **2007**, pp. 285–312.
6 A. N. Parikh, M. A. Schivley, E. Koo, K. Seshadri, D. Aurentz, K. Mueller, D. L. Allara, *J. Am. Chem. Soc.* **1997**, *119*, 3135.
7 A. Shimojima, Y. Sugahara, K. Kuroda, *Bull. Chem. Soc. Jpn.* **1997**, *70*, 2847.
8 R. Maoz, S. Matlis, E. DiMasi, B. M. Ocko, J. Sagiv, *Nature* **1996**, *384*, 150.
9 J. Minet, S. Abramson, B. Bresson, C. Sanchez, V. Montouillout, N. Lequeux, *Chem. Mater.* **2004**, *16*, 3955.
10 J. Sjoeblom, G. Stakkestad, H. Ebeltoft, S. E. Friberg, P. Claesson, *Langmuir* **1995**, *11*, 2652.
11 J. J. E. Moreau, B. P. Pichon, M. W. C. Man, C. Bied, H. Pritzkow, J.-L. Bantignies, P. Dieudonné, J. L. Sauvajol, *Angew. Chem., Int. Ed.* **2004**, *43*, 203.
12 J. Alauzun, A. Mehdi, C. Reyé, R. J. P. Corriu, *J. Mater. Chem.* **2005**, *15*, 841.
13 R. Mouawia, A. Mehdi, C. Reyé, R. J. P. Corriu, *J. Mater. Chem.* **2008**, *18*, 2028.
14 F. T. Yu, K. Yao, L. Y. Shi, H. Z. Wang, Y. Fu, X. Q. You, *Chem. Mater.* **2007**, *19*, 335.
15 J. Alauzun, E. Besson, A. Mehdi, C. Reyé, R. J. P. Corriu, *Chem. Mater.* **2008**, *20*, 503.
16 K. Yao, Y. Imai, L. Y. Shi, A. M. Dong, Y. Adachi, K. Nishikubo, E. Abe, H. Tateyama, *J. Colloid Interface Sci.* **2005**, *285*, 259.
17 T. Chujo, Y. Gonda, Y. Oumi, T. Sano, H. Yoshitake, *J. Mater. Chem.* **2007**, *17*, 1372.
18 Y. Kaneko, N. Iyi, T. Matsumoto, K. Fujii, K. Kurashima, T. Fujita, *J. Mater. Chem.* **2003**, *13*, 2058.
19 Y. T. Tao, *J. Am. Chem. Soc.* **1993**, *115*, 4350.
20 A. Burneau, J. P. Gallas, in *The Surface Properties of Silicas*, ed. by A. P. Legrand, John Wiley & Sons, Chichester, **1998**, pp. 175–178.
21 J. Neuefeind, K. D. Kiss, *Ber. Bunsen-Ges. Phys. Chem.* **1996**, *100*, 1341.
22 T. Charpentier, S. Ispas, M. Profeta, F. Mauri, C. J. Pickard, *J. Phys. Chem. B* **2004**, *108*, 4147.
23 A. K. Pant, *Acta Crystallogr., Sect. B* **1968**, *24*, 1077.
24 M. Sitarz, W. Mozgawa, M. Handke, *J. Mol. Struct.* **1999**, *511–512*, 281.